



ELSEVIER

Earth and Planetary Science Letters 133 (1995) 379–395

EP
SL

Incompatible trace elements in OIB and MORB and source enrichment in the sub-oceanic mantle

Alex N. Halliday^a, Der-Chuen Lee^a, Simone Tommasini^{a,1}, Gareth R. Davies^{a,1},
Cassi R. Paslick^a, J. Godfrey Fitton^b, Dodie E. James^b

^a Department of Geological Sciences, University of Michigan, Ann Arbor, MI 48109-1063, USA

^b Department of Geology and Geophysics, University of Edinburgh, Edinburgh EH9 3JW, UK

Received 21 February 1994; accepted 11 May 1995

Abstract

The concentrations of incompatible trace elements in ocean island basalts (OIB) from the central Atlantic extend to relatively enriched and fractionated compositions in regions of older oceanic lithosphere. Certain trace element ratios normally considered to be uniform in the mantle, such as Ce/Pb, are particularly variable. However, other trace element ratios that are expected to be variable because of differences in bulk distribution coefficient, such as Ce/U, are relatively uniform. The Ce/Pb ratios in enriched OIB are correlated with unusually high U/Pb and low K/U. These U/Pb ratios would have generated excessively radiogenic Pb if they were long-term (10^9 yr) features of the source such as might result from core formation or recycling of hydrothermally altered ocean floor basalts. However, volcanic centers with high U/Pb do have high $^{206}\text{Pb}/^{204}\text{Pb}$ for their $^{207}\text{Pb}/^{204}\text{Pb}$, a feature that is most easily modelled by enrichment in U relative to Pb about 10^8 yr prior to melting, a time similar to the age of the lithosphere. We propose that the source regions of these magmas are enriched by the introduction of small degree partial melts soon after the formation of the oceanic lithosphere. Metasomatism of the uppermost mantle by small degree partial melts produced in equilibrium with a combination of residual upper mantle major silicate phases, together with minor amphibole ($\leq 2\%$), sulfide ($\leq 0.2\%$) and phlogopite ($\leq 0.2\%$) at about the time of formation of the lithosphere, would generate a 'near-surface fractionated' (NSF) source with low K/U and high U/Pb, $\Delta^{206}\text{Pb}/^{204}\text{Pb}$ and Ce/Pb, while maintaining Ce/U, Nb/U, Ba/Ce and Ba/Nb that are only slightly fractionated relative to other OIB. An important feature of the modelling of NSF mantle is that U is more incompatible than Ba or Rb. This is confirmed by the variability in incompatible trace element ratios with U concentration for enriched OIB. However, this contrasts with the relative incompatibility deduced from U–Th–Ra disequilibrium data for MORB and OIB, endorsing the view that the variability in highly incompatible trace element ratios in enriched OIB is dominated by source enrichment effects that are distinct from the fractionation that takes place during the production of the erupted magmas.

The Ce/U, Ba/Ce and U/Pb ratios of all OIB, including enriched OIB from regions of old lithosphere, are uniform relative to data for MORB. This appears inconsistent with the degree of isotopic variability in OIB relative to MORB and is difficult to explain unless the variations in incompatible trace element ratios in MORB are dominated by effects other than melting. Ratio–element plots provide evidence that the incompatible element ratios of MORB are affected by OIB-component contamination in the source or in transit to the surface and this is consistent with covariation between trace element

¹ Present address: Faculteit der Aardwetenschappen, Vrije Universiteit, 1081 HV Amsterdam, The Netherlands

ratios and some isotopic compositions in MORB. The ratios and concentrations of highly incompatible trace elements in MORB vary as a consequence of this contamination, as well as degree of partial melting. The relative uniformity and near chondritic proportions of Ce/U and, to a lesser extent, Ba/Ce in OIB compared with MORB are difficult to reconcile with recycling models that advocate material resembling present-day MORB or hydrothermally altered MORB as the dominant component of OIB sources but are consistent with NSF mantle recycling. Similarly, the Ba/U/Ce ratios are inconsistent with models in which the OIB source was affected by Ca perovskite fractionation in a magma ocean on the early Earth.

1. Introduction

The relative concentrations of incompatible trace elements in Earth's mantle provide critical clues for our understanding of accretion history, core formation, the growth of the crust, recycling via subduction, melt processes and the scales and causes of mantle heterogeneity. A significant advance in this subject area over the past few years has involved empirical estimates of relative bulk distribution coefficients and source compositions based on high-quality compositional data for carefully screened and selected basalt samples [1–5]. If the concentration ratio of two incompatible elements is independent of concentration it is argued that they have the same value of D —the bulk distribution coefficient [6]. This method of determining the degree of incompatibility of trace elements is often the best approach available and is, for example, the method used to estimate the K/U ratio in the upper mantle, upon which calculations of heat production are based [1], and the Ce/Pb ratio which places important constraints on the history of recycling in the mantle [3]. Nevertheless, some of the ratios that have originally been thought on this basis to be uniform in the mantle have subsequently been shown to vary significantly [5,7].

This study presents new trace element data for basaltic lavas from ocean islands in the central Atlantic. Certain supposedly uniform trace element ratios in ocean island basalts (OIB) are fractionated in regions of old oceanic lithosphere. This appears to be caused by metasomatic enrichment in the sub-oceanic upper mantle at the time of formation of the lithosphere. However, certain other incompatible trace element ratios, which can be expected to be quite variable in basalts generally (Ce/U, Ba/Ce), appear to be relatively uniform, even in highly enriched OIB. In fact, OIB is more uniform in many

incompatible trace element ratios than mid-ocean ridge basalts (MORB), the opposite of that anticipated from the relative degrees of heterogeneity in isotopic compositions. Hence, the differences between the variability in MORB and OIB reflect distinct mantle processes for the two magma types and place significant constraints on the recent history of melting and source enrichment, as well as the generation of global scale mantle heterogeneity.

2. Approach

The central Atlantic is excellent for studying basalt compositions as a function of degree of partial melting because the region is removed from the complicating effects of the DUPAL anomaly in the southern hemisphere [8] and there are no recent subduction zones nearby. The central Atlantic includes a number of islands with basalts of very different composition in old (thick) and young (thin) lithosphere [9–12]. The current database for combined trace element and isotopic compositions of lavas from this region is fragmented. Consequently we have attempted to bridge some of the gaps with a reconnaissance study that complements published trace element studies of the Cameroon line [13,14], the Azores [7], St. Helena [15] and the Cape Verdes [16]. The new results are presented in Table 1 and include data for Ascension, Madeira, Fernando de Noronha, Trindade, the Cameroon line oceanic and continent/ocean boundary (COB) sectors and some of the Azores islands for which few data have been published. All of these lavas are < 10 Ma in age, petrographically relatively fresh and contain more than 4 wt% MgO. The Nd, Sr and Pb isotope geochemistry of these samples are presented elsewhere [7,9,16–18,20].

Major and trace element analyses were deter-

mined using XRF at the University of Edinburgh, deploying techniques described previously [13]. All concentrations of U and Pb, and some Rb, Sr and

REE concentrations, were determined by isotope dilution TIMS using techniques outlined elsewhere [19]. Nearly all the ID measurements should be

Table 1
Concentrations of incompatible trace elements in central Atlantic OIB

| Sample Number | MgO wt% | Rb ppm | Ba ppm | K wt% | U ppm | Nb ppm | La ppm | Ce ppm | Pb ppm | Sr ppm | P ppm | Nd ppm | Sm ppm | Zr ppm | Eu ppm | Ti ppm | Gd ppm | Dy ppm | Y ppm | Er ppm | Yb ppm | Lu ppm |
|------------------------------------|---------|--------|--------|-------|-------|--------|--------|--------|--------|--------|-------|--------|--------|--------|--------|--------|--------|--------|-------|--------|--------|--------|
| <i>Azores - Pico</i> | | | | | | | | | | | | | | | | | | | | | | |
| AZP6 | 6.2 | 27 | 359 | 1.12 | 1.23 | 55 | 39 | 100 | 2.75 | 734 | 0.34 | 54 | | 306 | | 2.19 | | | | | | 32 |
| AZP7 | 16.1 | 12 | 197 | 0.52 | 0.443 | 20 | 17 | 33 | 1.70 | 303 | 0.12 | 21 | | 113 | | 1.00 | | | | | | 18 |
| AZP8 | 13.2 | 19 | 261 | 0.79 | 0.701 | 29 | 17 | 52 | 2.32 | 444 | 0.14 | 26 | | 160 | | 1.21 | | | | | | 21 |
| <i>Azores - Flores</i> | | | | | | | | | | | | | | | | | | | | | | |
| AZF1 | 4.8 | 44.2 | 812 | 1.59 | 1.38 | 83 | 69.2 | 116 | 3.03 | 736 | 0.38 | 51.9 | 9.50 | 249 | 3.19 | 1.47 | 8.46 | 6.49 | 32 | 3.26 | 2.64 | |
| AZF2 | 6.1 | 47.9 | 696 | 1.44 | 1.45 | 85 | 67.9 | 111 | 3.63 | 767 | 0.29 | 45.7 | 8.26 | 291 | 2.62 | 1.49 | 7.55 | 5.51 | 27 | 2.77 | 2.25 | |
| <i>Azores - Fayal</i> | | | | | | | | | | | | | | | | | | | | | | |
| AZFY2 | 10.2 | 24.9 | 312 | 0.82 | 0.644 | 33 | 26.3 | 54.9 | 1.96 | 543 | 0.17 | 28.9 | 6.37 | 183 | 2.08 | 1.60 | 6.30 | 5.00 | 25 | 2.42 | 1.89 | |
| AZFY3 | 8.6 | 44.9 | 391 | 1.09 | 1.07 | 43 | 36.5 | 73.1 | 7.03 | 631 | 0.21 | 35.3 | 7.30 | 239 | 2.33 | 1.65 | 6.81 | 5.31 | 27 | 2.52 | 1.97 | |
| <i>Cameroon Line - São Tomé</i> | | | | | | | | | | | | | | | | | | | | | | |
| ST19 | 5.5 | 60 | 728 | 1.81 | 2.86 | 99 | 83 | 163 | 5.44 | 1113 | 0.44 | 68.5 | 13.2 | 472 | | 2.26 | | | | | | 36 |
| ST72 | 8.3 | 46 | 722 | 1.20 | | 93 | 81 | 160 | | 1130 | 0.45 | | | 367 | | 1.90 | | | | | | 33 |
| ST83 | 4.8 | 8 | 799 | 0.80 | | 114 | 97 | 196 | | 1174 | 0.55 | | | 490 | | 2.31 | | | | | | 43 |
| ST96 | 4.1 | 62 | 854 | 2.31 | 2.04 | 105 | 89 | 180 | 4.72 | 1056 | 0.43 | 70.9 | 12.9 | 527 | | 1.50 | | | | | | 37 |
| ST106 | 13.2 | 29 | 528 | 0.98 | | 62 | 56 | 112 | | 836 | 0.36 | | | 273 | | 1.68 | | | | | | 28 |
| ST107 | 6.3 | 62 | 750 | 1.79 | 3.28 | 103 | 89 | 168 | 5.86 | 1102 | 0.33 | 63.2 | 11.5 | 501 | | 1.75 | | | | | | 32 |
| ST109 | 9.1 | 29 | 452 | 1.05 | | 60 | 49 | 98 | | 824 | 0.28 | | | 282 | | 1.78 | | | | | | 28 |
| <i>Cameroon Line - Príncipe</i> | | | | | | | | | | | | | | | | | | | | | | |
| P17 | 11.0 | 30 | 397 | 0.97 | 1.00 | 51 | 42 | 87 | 2.22 | 765 | 0.25 | 40.3 | 8.37 | 231 | | 1.75 | | | | | | 24 |
| P19 | 8.9 | 43 | 684 | 1.61 | 1.58 | 78 | 71 | 140 | 3.11 | 1153 | 0.46 | 57.6 | 11.1 | 320 | | 2.10 | | | | | | 33 |
| <i>Cameroon Line - Bioko</i> | | | | | | | | | | | | | | | | | | | | | | |
| FP1 | 8.1 | 26 | 449 | 0.95 | 1.07 | 56 | 44 | 100 | 2.76 | 726 | 0.23 | 45.6 | 9.67 | 288 | | 2.21 | | | | | | 30 |
| FP23 | 9.4 | 26 | 406 | 0.93 | | 61 | 60 | 126 | | 685 | 0.23 | | | 298 | | 2.23 | | | | | | 28 |
| FP32 | 4.3 | 61 | 836 | 1.70 | | 119 | 99 | 200 | | 1199 | 0.38 | | | 393 | | 2.05 | | | | | | 40 |
| FP38 | 10.8 | 25 | 353 | 0.80 | 0.775 | 47 | 41 | 87 | 2.54 | 647 | 0.21 | 40.5 | 8.79 | 274 | | 2.02 | | | | | | 28 |
| FP44 | 10.8 | 33 | 562 | 0.98 | 1.44 | 65 | 58 | 121 | 3.07 | 823 | 0.28 | 48.7 | 9.72 | 336 | | 2.11 | | | | | | 32 |
| <i>Cameroon Line - Etinde</i> | | | | | | | | | | | | | | | | | | | | | | |
| C24 | 5.3 | 87 | 1067 | 2.17 | 5.69 | 223 | 238 | 489 | 7.56 | 2401 | 0.52 | 176 | 25.1 | 656 | | 2.43 | | | | | | 47 |
| C150 | 8.0 | 89 | 788 | 1.38 | 2.45 | 96 | 97 | 197 | 3.84 | 1054 | 0.29 | 89.6 | 14.3 | 399 | | 2.69 | | | | | | 28 |
| <i>Cameroon Line - Mt Cameroon</i> | | | | | | | | | | | | | | | | | | | | | | |
| C1 | 5.4 | 43 | 599 | 1.49 | 2.83 | 103 | 87 | 182 | 4.46 | 1136 | 0.36 | 74.6 | 12.9 | 407 | | 1.90 | | | | | | 36 |
| C5 | 4.2 | 51 | 650 | 1.73 | | 118 | 97 | 199 | | 1202 | 0.40 | | | 461 | | 1.76 | | | | | | 38 |
| C25 | 10.5 | 36 | 479 | 1.16 | 2.13 | 92 | 83 | 164 | 3.75 | 989 | 0.32 | 68.9 | 11.9 | 356 | | 1.84 | | | | | | 29 |
| C195 | 6.2 | 29 | 414 | 1.05 | 1.56 | 72 | 59 | 129 | 2.98 | 885 | 0.24 | | | 307 | | 2.02 | | | | | | 29 |
| C197 | 5.9 | 33 | 443 | 1.16 | 1.77 | 81 | 66 | 143 | 3.46 | 974 | 0.27 | | | 335 | | 2.06 | | | | | | 30 |
| C199 | 5.8 | 34 | 456 | 1.17 | 1.78 | 82 | 70 | 140 | | 976 | 0.27 | | | 340 | | 2.04 | | | | | | 32 |
| C200 | 6.2 | 32 | 404 | 1.08 | 1.63 | 74 | 59 | 131 | 2.89 | 903 | 0.24 | | | 312 | | 2.03 | | | | | | 30 |
| C212 | 5.9 | 33 | 453 | 1.19 | 1.83 | 83 | 68 | 147 | 2.7 | 985 | 0.27 | | | 343 | | 2.04 | | | | | | |
| <i>Ascension</i> | | | | | | | | | | | | | | | | | | | | | | |
| AS3 | 5.3 | 18.7 | 310 | 0.97 | 0.758 | 42 | 30.4 | 66.8 | 2.19 | 449 | 0.37 | 37.9 | 8.77 | 224 | 2.92 | 2.07 | | | 7.5 | 37 | 3.78 | |
| AS5 | 4.2 | 27.1 | 402 | 1.31 | 1.21 | 63 | 45.3 | 101 | 2.66 | 449 | 0.64 | 56.9 | 12.8 | 318 | 4.16 | 1.74 | | | 10.5 | 52 | 5.28 | |
| AS10 | 4.6 | 24.0 | 386 | 1.17 | 0.901 | 53 | 37.5 | 79.5 | 2.62 | 592 | 0.40 | 40.7 | 8.90 | 311 | 3.04 | 1.96 | | | 7.14 | 36 | 3.62 | |
| <i>Madeira</i> | | | | | | | | | | | | | | | | | | | | | | |
| MD4 | 6.5 | 23.5 | 366 | 0.84 | 1.37 | 65 | 63.3 | 108 | 2.49 | 781 | 0.31 | 50.0 | 9.74 | 303 | 3.02 | 1.73 | 9.04 | 6.55 | 31 | 3.14 | 2.13 | 0.359 |
| MD10 | 7.5 | 23.2 | 370 | 0.81 | 1.3 | 65 | 62.8 | 112 | 2.8 | 860 | 0.32 | 53.6 | 10.6 | 307 | 3.31 | 1.76 | 9.85 | 7.16 | 34 | 3.41 | 2.39 | 0.382 |
| MD40 | 10.7 | 15.2 | 231 | 0.59 | 0.675 | 34 | 27.2 | 58.8 | 1.46 | 541 | 0.19 | 31.1 | 6.73 | 185 | 2.19 | 1.51 | 6.63 | 5.04 | 25 | 2.42 | 1.69 | 0.260 |
| MD64 | 8.1 | 23.6 | 357 | 0.75 | 1.33 | 65 | 51.2 | 105 | 2.39 | 814 | 0.41 | 51.4 | 10.1 | 303 | 3.15 | 1.65 | 9.52 | 6.71 | 31 | 3.16 | 2.27 | 0.344 |
| <i>Fernando de Noronha</i> | | | | | | | | | | | | | | | | | | | | | | |
| FDN25 | 10.7 | 31.7 | 283 | 1.04 | 1.01 | 37 | 30 | 76 | 3.02 | 567 | 0.18 | 39.6 | 8.48 | 249 | | 2.06 | | | | | | 25 |
| FDN55 | 5.6 | 79 | 1094 | 1.98 | 5.28 | 100 | 125 | 233 | 9.16 | 1383 | 0.49 | 87 | | 452 | | 1.96 | | | | | | 36 |
| FDN72 | 8.3 | 65.2 | 707 | 2.26 | | 83 | 87 | 145 | | 1162 | 0.21 | 45.2 | 7.78 | 395 | | 1.22 | | | | | | 25 |
| FDN20 | 12.8 | 56.2 | 956 | 1.68 | 2.38 | 123 | 73 | 148 | 14.5 | 1641 | 0.49 | 91.4 | 16.2 | 427 | | 2.63 | | | | | | 31 |
| FDN36 | 10.7 | 26.5 | 428 | 0.96 | 1.85 | 63 | | 98 | 3.09 | 769 | | 48.8 | 9.71 | | | | | | | | | |
| FDN71 | 7.9 | 45.7 | 513 | 1.29 | | 71 | | 120 | | 859 | | 55.1 | 10.4 | | | | | | | | | |
| FDN79 | 9.3 | 75 | 961 | 2.07 | 4.19 | 102 | | 184 | 7.7 | 1777 | | 65.2 | 12 | | | | | | | | | |
| <i>Trinidad</i> | | | | | | | | | | | | | | | | | | | | | | |
| TD3 | 13.4 | 39 | 657 | 1.44 | 0.917 | 64 | 36 | 79 | 2.20 | 690 | 0.21 | 36.7 | 7.2 | 253 | | 1.91 | | | | | | 20 |
| TD4 | 5.6 | 60 | 1058 | 1.06 | 4.01 | 165 | 170 | 379 | 4.31 | 2511 | 1.40 | 170 | 22.3 | 749 | | 2.57 | | | | | | 63 |

All data obtained by XRF and ID (TIMS) as follows: All Ba, K, Nb, P, Zr, Ti and Y by XRF. All U, Pb, Eu, Gd, Dy, Er, Yb and Lu by ID. All Rb and Sr by ID except Azores–Pico, Cameroon line and Trinidad. All La and Ce by ID except Azores–Pico, Cameroon line, Trinidad and Fernando de Noronha. All Nd and Sm by ID except Azores–Pico and FDN25. ID data for Fernando de Noronha from [17]. ID data for Cameroon line samples are from [18–20]. Corresponding Nd, Sr and Pb isotopic compositions for all samples are from [9,17–20]. U and Pb concentrations for Madeira are new determinations and do not correspond to $^{238}\text{U}/^{204}\text{Pb}$ reported in [9].

accurate to within $\pm 1\%$. Our ID and XRF analyses for La, Ce and Nd always agree to within better than $\pm 30\%$. XRF accuracy for Rb and Sr is better than $\pm 5\%$, for Ba, Nb and Zr it is considered better than $\pm 20\%$. These uncertainties are insignificant in terms of the trends displayed by the data and their interpretation.

We have also used relevant data in the literature for other samples for which isotope dilution U and Pb data were available [1–3,45,7,9,16–26]. The MORB trace element and isotopic data are only for samples of fresh glasses from the Atlantic, Pacific and Indian Oceans, for which U, Pb and Ce analyses were published by the Mainz group in [1,3,4]. These are generally regarded as N-MORB. Screening analyses of OIB has been more complicated. Even in reasonably fresh OIB the tendency for mobility of certain elements (Rb, Ba, U, Pb) needs to be evalu-

ated. In this study we find that U and Ba to LREE ratios are surprisingly *uniform* in OIB and hence the question of heterogeneity produced by mobility of U does not normally arise. Hofmann and White [2] showed that Ba/Rb was very sensitive to alteration. We have therefore screened the data and excluded all samples if the Ba/Rb ratio is < 5 or > 20 . Even after this screening it was found that some of the trace element data for Tubuai [22] are particularly scattered and we have therefore further excluded three samples with anomalous Nb/U, Ce/U, K/U and Ba/Ce. Finally, we have included in this study a suite of basaltic lavas collected during or soon after the 1982 eruption of Mt. Cameroon [18–20]. These show the same extreme trends in Ce/Pb, U/Pb and K/U as other samples, thereby demonstrating that the trends are not the result of U, Pb or K mobility during alteration.

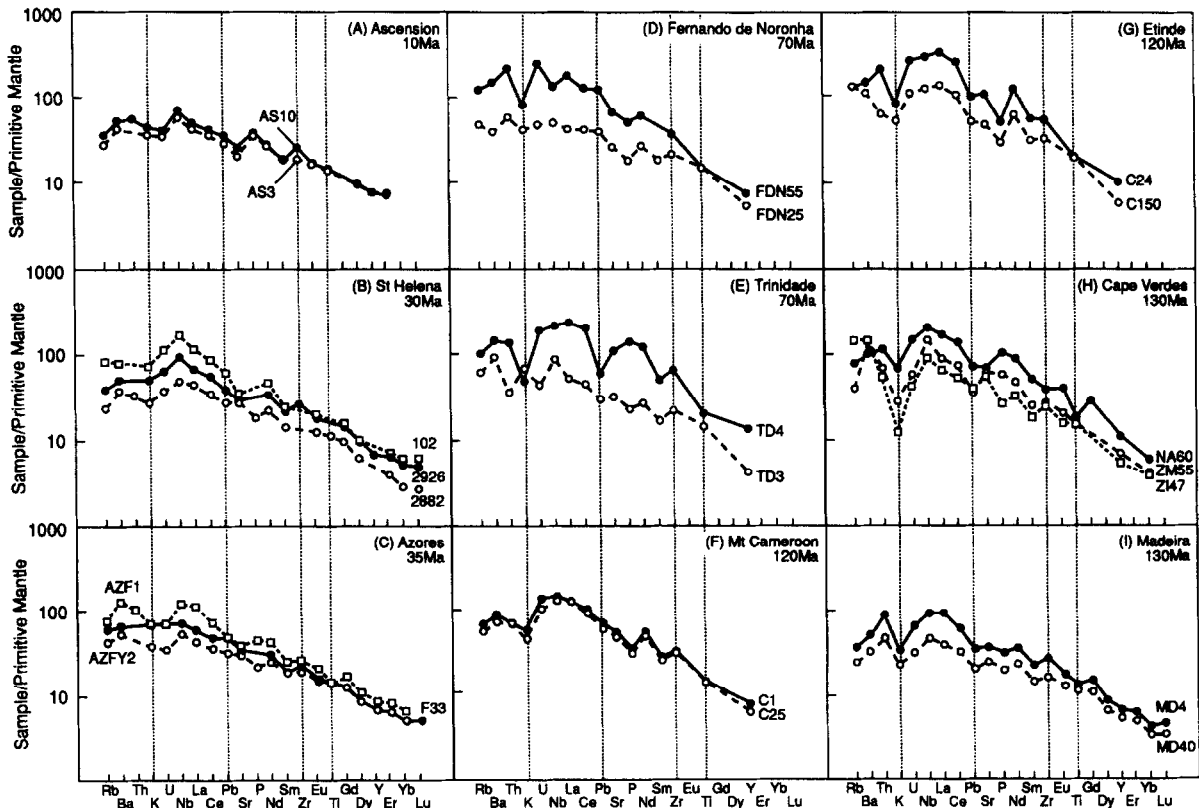


Fig. 1. Incompatible trace element concentrations normalized to values for primitive mantle for different central Atlantic islands with the approximate age of the ocean floor [10–12] noted for each island. There is a more marked depletion in K and Pb in areas of old lithosphere. Data from Table 1 and [4,5,7,16,17].

3. Fractionation of U, Ce, Pb, K and Ba in the Earth's mantle

Representative plots of the incompatible trace element concentrations for the different central Atlantic islands normalized to primitive mantle [5] are presented in Fig. 1. The island closest to the Mid-Atlantic Ridge in the area with the youngest lithosphere (< 10 Ma) is Ascension. The data for Ascension define relatively flat normalized plots (Fig. 1A) with depletion of Sr, which is probably the result of minor plagioclase fractionation. The Azores and St. Helena are located in slightly older lithosphere (35 and 30 Ma respectively). The Azores patterns are also relatively flat (Fig. 1B) but the St. Helena data show a characteristic enrichment in Nb relative to other incompatible elements [5,15] and a slight de-

pletion in K (Fig. 1C). Fernando da Noronha is located in 70 Ma lithosphere and shows a more extreme depletion in K (Fig. 1D). The remaining volcanic centers, all in areas of old lithosphere, Madeira (130 Ma), Cape Verdes (130 Ma), Trindade (70 Ma) and the COB of the Cameroon line (Mt. Cameroon and Etinde, 120 Ma), display extreme depletion in K and variable depletion in Pb. Some of these display relative enrichment in Zr and depletion in Ti relative to the adjacent REEs. The Mt. Cameroon and Etinde samples are depleted in P, possibly reflecting a small amount of apatite in the source. Generally speaking (and there are exceptions), lavas erupted further away from the Mid-Atlantic Ridge are more LREE enriched and are depleted in K and Pb relative to Ba, Th, U, Nb and the LREEs. However, even in the most extreme

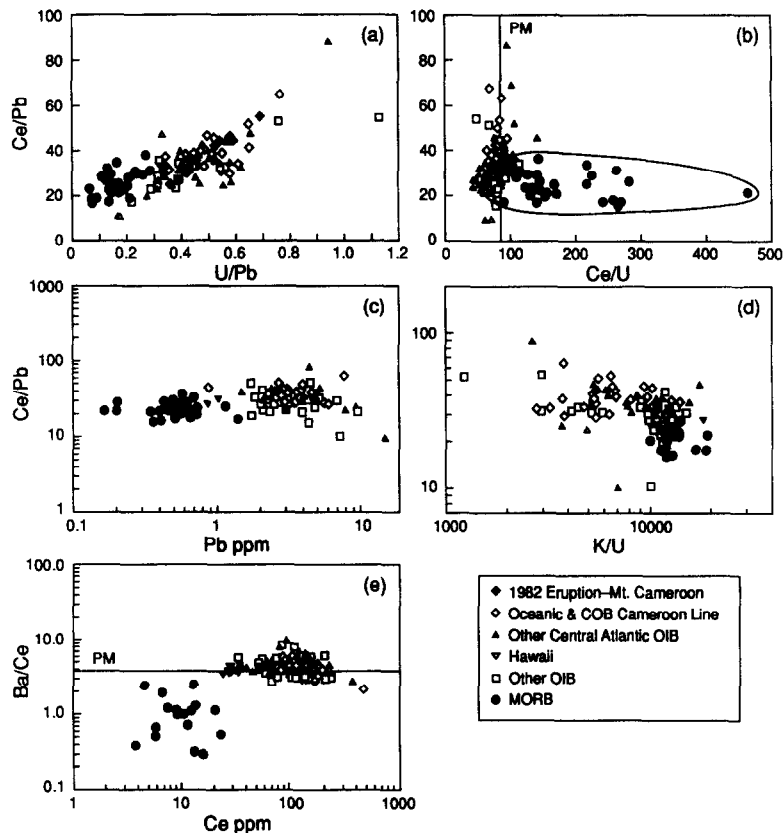


Fig. 2. Plots of Ce/Pb vs. (a) U/Pb, (b) Ce/U, (c) Pb concentration and (d) K/U, and (e) a plot of Ba/Ce against Ce concentration, for MORB and OIB. Compilation includes data for Atlantic, Pacific and Indian Ocean MORB glasses, and Ascension, Azores, Bioko, Cape Verdes, Comoros, Etinde, Fernando de Noronha, Gough, Hawaii, Madeira, Mt. Cameroon, Pagalu, Principe, Reunion, St. Helena, Samoa, São Tomé, Trindade, Tristan da Cunha and Tubuai. PM = primitive mantle. Data from Table 1 and [1–5,7,16,21,22,25].

examples of K depletion (e.g., Etinde and Trinidad), the ratios of Ba and U to La and Ce are approximately constant, and roughly equivalent to the chondritic proportions expected in primitive mantle. The details and causes of these features are now addressed with the use of trace element ratio plots.

The Ce/Pb ratios of MORB and OIB are generally considered to be relatively uniform, implying that the bulk *D*s for Ce and Pb are the same, as argued by Hofmann et al. [3]. As such the Ce/Pb ratios of OIB should be essentially independent of trace element ratios such as U/Pb, which vary greatly, presumably because U is more incompatible than Pb [4]. On combining the data for the central Atlantic islands with other high-quality published data we see a surprisingly large range in Ce/Pb (15–90), and positive correlation with U/Pb (Fig. 2a) but not with Pb (Fig. 2c). The trend of the data in Fig. 2a appears to be mainly influenced by the data for samples from Cape Verdes, Trinidad, Tubuai and the oceanic and COB sections of the Cameroon line. This trend is not caused by alteration. Alkali basalts collected at the time of the eruption of Mt. Cameroon in 1982 yield both high U/Pb (~0.5) and Ce/Pb (40–50), as shown in Fig. 2a. There is complete overlap between the Ce/Pb ratios of fresh MORB glasses and OIB with low U/Pb. Only two samples, one from Fernando de Noronha [17] and one from the Azores [7], have Ce/Pb slightly lower than that found in MORB. Considerable evidence exists that U is more incompatible than Pb in mantle melting [4,19,22,27–32]. It might seem tempting to conclude, therefore, that Ce is slightly more incompatible than Pb in OIB melting. However, this does not find support in published partition coefficients

for clinopyroxene and garnet, the most likely major phases to control such trace element ratios in mantle melting [27–35]. There should also be a negative relationship between Ce/Pb and Ce/U if Ce is more incompatible than Pb because U is more incompatible than Ce. In fact, the Ce/U ratios in MORB display a large range (Fig. 2b), and are not correlated with Ce/Pb, which is relatively uniform. In contrast, in the case of OIB it is the Ce/Pb ratios that are more variable (by a factor of 6) and these are not correlated with Ce/U ratios (which vary by only a factor of 3). The relative standard errors from the mean (RSEM) for the data shown in Fig. 2 are given in Table 2. It can be seen that MORB Ce/U and U/Pb ratios for the same suite of samples have the same RSEM (0.44), entirely consistent with uniform Ce/Pb in the MORB source (RSEM = 0.21). In contrast, despite the smaller dataset for MORB, U/Pb is more uniform in OIB (RSEM = 0.34). Furthermore, in contrast to MORB, U/Pb shows variability similar to that for Ce/Pb (RSEM = 0.32). This is a little greater than the RSEM for Ce/U (0.29), which is significantly less than the RSEM for Ce/U in MORB (0.44). The Cameroon line is somewhat unusual in its setting [14,18–21] and in order to demonstrate that this is not unduly influencing the statistics, the relative variability defined by the OIB dataset without the Cameroon line is also shown (Table 2). The changes in all the trace element ratio means are negligible. The biggest changes in variance are *increases* for U/Pb (RSEM = 0.39) and Ce/Pb (RSEM = 0.36) and a decrease for K/U (RSEM = 0.45).

These data present something of a paradox. In the simplest melting models and assuming a uniform

Table 2

Mean and standard errors from the mean for incompatible trace element ratios in MORB and OIB

| Ratio | Primitive | MORB | | OIB | | OIB (less Cameroon) | |
|-------|-----------|----------------|-------|---------------|-------|---------------------|-------|
| | Mantle | Mean ± σ | σ (%) | Mean ± σ | σ (%) | Mean ± σ | σ (%) |
| U/Pb | 0.11 | 0.16 ± 0.07 | 44 | 0.45 ± 0.15 | 34 | 0.43 ± 0.17 | 39 |
| Ce/Pb | 25 | 24 ± 5 | 21 | 35 ± 11 | 32 | 33 ± 12 | 36 |
| Ce/U | 85 | 180 ± 79 | 44 | 88 ± 26 | 29 | 90 ± 29 | 32 |
| Ba/Ce | 3.9 | 1.1 ± 0.6 | 60 | 4.5 ± 1.3 | 30 | 4.6 ± 1.5 | 32 |
| Ba/Nb | 9.8 | 3.5 ± 1.6 | 46 | 7.9 ± 2.3 | 29 | 8.0 ± 2.5 | 31 |
| K/U | 11,900 | 12,700 ± 2,300 | 18 | 9,800 ± 4,800 | 49 | 10,900 ± 4,900 | 45 |
| Nb/U | 34 | 49 ± 9 | 18 | 48 ± 11 | 23 | 49 ± 11 | 22 |

Primitive mantle values from [5].

source, incompatible trace element ratios are expected to vary with degree of partial melting as a function of differences in bulk distribution coefficient [6]. The degree of fractionation in the melt should decrease with increasing degree of partial melting. Hence if Ce/U is more uniform in OIB than MORB either (a) the OIB source is more uniform than the MORB source, which on isotopic grounds would appear unlikely, or (b) the degree of partial melting in OIB is larger than it is in MORB such that Ce/U is unfractionated in the former but fractionated in the latter, which runs contrary to traditional thinking based on the experimental petrology of basalt, or (c) OIB melt fractions are very uniform, which given the range of trace element concentrations in OIB appears implausible, or (d) the variabilities in Ce/U/Pb imparted to MORB and OIB are the products of processes other than fractionation during melting. A similar problem for other incompatible trace element ratios has been noted by Allègre et al. [36].

The decoupling of U–Pb from other isotopic systems has been discussed previously (e.g., [37]). Therefore, the correlated behavior of Ce/Pb and U/Pb in OIB, but lack of relationship with Ce/U, might be thought to implicate a process that affects Pb preferentially, totally unrelated with melting, such as core formation [38] or recycling of oceanic crust depleted in Pb by hydrothermal scavenging [39]. However, if the large-scale composition of the mantle is being affected in this manner it is unclear why such Pb-depleted reservoirs should be more apparent in the Madeira, Cape Verdes, Trinidad and Cameroon line basalts, from areas of old lithosphere. Furthermore, the high U/Pb ratios characteristic of these magmas would produce *extremely* radiogenic lead if they were long-term features of their sources that were allowed to evolve for longer than the age of the lithosphere (10^8 yr). Hence they cannot be the products of processes such as core formation, or recycling of hydrothermally depleted lithosphere [9,19]. This is illustrated in Fig. 3, which shows the Pb isotopic compositions of mantle that has been fractionated in U/Pb to varying degrees and compares these with normal Pb isotopic compositions of oceanic basalts. The arrays are constructed assuming that ‘typical mantle’ is defined by the ‘northern hemisphere reference line’ (NHRL) of Hart [8]. This

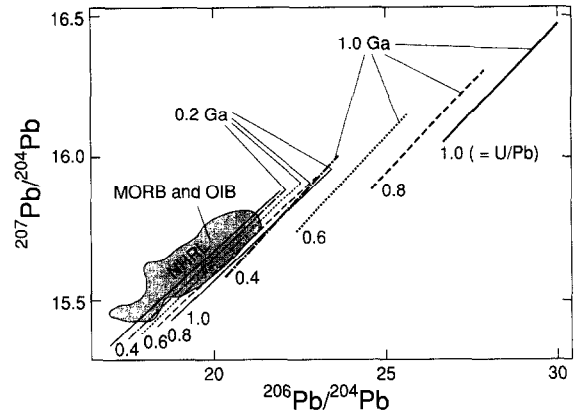


Fig. 3. The calculated effects of high U/Pb, such as is measured for some erupted lavas, on Pb isotopic heterogeneity, if these were long-term features of OIB and MORB sources. The lines are model values for the NHRL [8], if the mantle sources for MORB and OIB had been fractionated in U/Pb to the various degrees shown at 0.2 and 1.0 Ga. See text for discussion.

is arbitrary and does not affect the outcome of the model. The μ for such ‘typical’ mantle is further assumed to vary linearly from 5 to 15 between $^{206}\text{Pb}/^{204}\text{Pb} = 17$ and 22. The effect on the NHRL of an increase in U/Pb to 0.4, 0.6, 0.8 and 1.0 (μ of 25, 38, 50 and 63) at 1.0 and 0.2 Ga is shown in Fig. 3. It is clear that U/Pb ratios corresponding to those observed in the lavas cannot be long-term features of the asthenosphere and must be destroyed or diluted by mixing with low-U/Pb mantle. Therefore, while the process that fractionates Ce/Pb and U/Pb does not fractionate Ce/U, it must be a relatively young feature [9,19].

While lead isotope data are inconsistent with long-term high U/Pb in the mantle, there is evidence that high U/Pb has been a feature of the source regions of the high U/Pb lavas for periods of the order of 10^8 yr. There is a small but significant increase in $^{206}\text{Pb}/^{204}\text{Pb}$ relative to $^{207}\text{Pb}/^{204}\text{Pb}$ that is consistent with an increase in U/Pb within the upper mantle at about the time of formation of the lithosphere [9,19]. This is illustrated in Fig. 4, in which $\Delta^{206}\text{Pb}/^{204}\text{Pb}$ is plotted against U/Pb for the same suite of samples, averaged by location. $\Delta^{206}\text{Pb}/^{204}\text{Pb}$ is defined as the deviation of $^{206}\text{Pb}/^{204}\text{Pb}$ from the NHRL of Hart [8], and by definition is inversely correlated with the results for Hart’s expression for $\Delta^{207}\text{Pb}/^{204}\text{Pb}$. It provides a

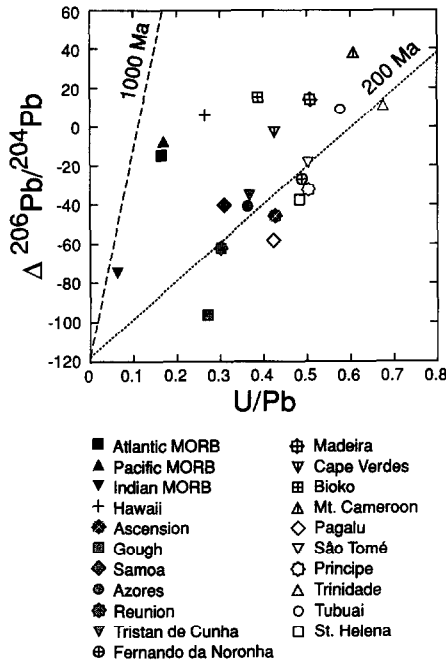


Fig. 4. $\Delta^{206}\text{Pb}/^{204}\text{Pb}$ is defined as the deviation of $^{206}\text{Pb}/^{204}\text{Pb}$ from the NHRL of Hart [8], and by definition is inversely correlated with the results for Hart's expression for $\Delta^{207}\text{Pb}/^{204}\text{Pb}$. $\Delta^{206}\text{Pb}/^{204}\text{Pb}$ is plotted against U/Pb for the same suite of samples, averaged by location. The calculated effects of high U/Pb, such as is measured for some erupted lavas, on Pb isotopic heterogeneity, if these were short-term and young features of OIB and MORB sources, is to increase $^{206}\text{Pb}/^{204}\text{Pb}$ relative to $^{207}\text{Pb}/^{204}\text{Pb}$ and hence increase $\Delta^{206}\text{Pb}/^{204}\text{Pb}$. The amount of time corresponding to the differences in $^{206}\text{Pb}/^{204}\text{Pb}$ for a given U/Pb is marked with the reference lines. Data from Table 1 and [1–5,7,9,16–26]. See text for discussion.

parameter quantifying the degree of scatter in $^{206}\text{Pb}/^{204}\text{Pb}$ when $^{207}\text{Pb}/^{204}\text{Pb}$ is plotted against it. A possible reason for such scatter is young ($\sim 10^8$ yr) extreme enrichment in U/Pb. Ancient enrichment would also result in major increases in $^{207}\text{Pb}/^{204}\text{Pb}$ (Fig. 3) whereas if the fractionation in U/Pb is young there would be a greater increase in $^{206}\text{Pb}/^{204}\text{Pb}$ relative to $^{207}\text{Pb}/^{204}\text{Pb}$, and therefore in $\Delta^{206}\text{Pb}/^{204}\text{Pb}$. The choice of particular reference line is not critical to this argument. Using a best-fit regression line produces a similar effect. It can be seen that $\Delta^{206}\text{Pb}/^{204}\text{Pb}$ is higher in regions with lavas with high U/Pb. Overall, the data define a rather broad trend with MORBs having relatively low U/Pb and $\Delta^{206}\text{Pb}/^{204}\text{Pb}$, and high

$\Delta^{206}\text{Pb}/^{204}\text{Pb}$ for their U/Pb. DUPAL centers such as Tristan da Cunha and Gough have very low $\Delta^{206}\text{Pb}/^{204}\text{Pb}$ and U/Pb, consistent with recycling of continental crust with high $\Delta^{207}\text{Pb}/^{204}\text{Pb}$ and low U/Pb [8]. Centers with high U/Pb (Mt. Cameroon, Trinidad, Madeira, Tubuai) have high $\Delta^{206}\text{Pb}/^{204}\text{Pb}$. The simplest explanation for this is that the high U/Pb is a feature of the source. In order to develop the differences in $^{206}\text{Pb}/^{204}\text{Pb}$ with the high U/Pb measured for the lavas (i.e., assuming little or no fractionation during melting) would require timespans of the order of only 10^8 yr (as shown in Fig. 4). The Atlantic centers with high U/Pb and high $\Delta^{206}\text{Pb}/^{204}\text{Pb}$ (Mt. Cameroon, Trinidad, Madeira) are therefore probably tapping sources fractionated in U/Pb in the relatively recent ($\sim 10^8$ yr) past. Some sources, such as Tubuai, may

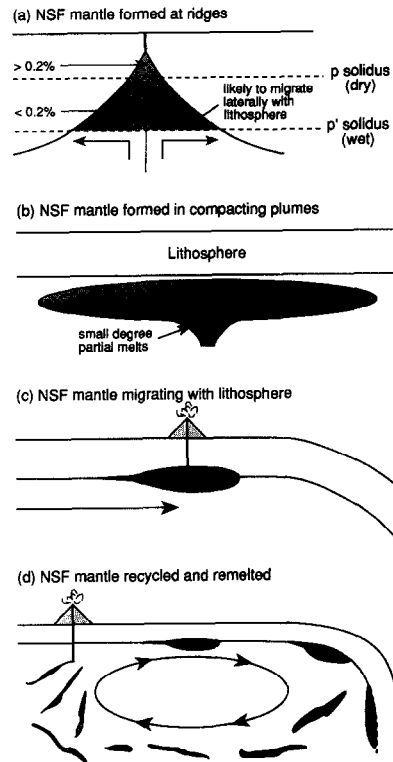


Fig. 5. Cartoons illustrating the types of mechanisms that may be responsible for producing near-surface fractionated (NSF) mantle near (a) ridges [40,41] and (b) plumes [19,42,43], and the (c) short (10^8 yr) and (d) long (10^9 yr) term consequences of such NSF mantle on OIB sources. p' = peridotite wet solidus; p = peridotite dry solidus.

have already had moderately elevated U/Pb prior to this time, and this would contribute to their overall high $^{207}\text{Pb}/^{204}\text{Pb}$ as well as high $^{206}\text{Pb}/^{204}\text{Pb}$. However, the high $\Delta^{206}\text{Pb}/^{204}\text{Pb}$ is probably not the product of such long-term recycling alone, and the very high average U/Pb of the lavas cannot be a long-term feature of the source (Fig. 3). Neither can the high U/Pb simply be the result of the partial melting that generated the sampled lavas (Fig. 4).

That U/Pb and $\Delta^{206}\text{Pb}/^{204}\text{Pb}$ tend to be higher in the source regions of lavas from regions of old lithosphere, and that the time scales required for this are of the order of 10^8 yr, is consistent with fractionation in U/Pb (and Ce/Pb) around the time of formation of new lithosphere. The fractionation in Ce/Pb and U/Pb in the upper mantle may be caused by metasomatic enrichment via small degree partial melts, such as those that may form between the wet and dry solidi (p' and p in Fig. 5) of mantle peridotite near ridges [40,41]. The melts that enrich the source region and produce this 'near-surface fractionated' (NSF) mantle would need to form in the presence of critical residual phases that fraction-

ate Pb relative to Ce and U by partitioning during low degree partial melting. With the exception of Madeira and Ascension [9] it is clear from Nd and Sr isotopic data that the central Atlantic islands are not derived from MORB-like sources. The source regions also involve less depleted heterogeneous material, dispersed in the asthenosphere or accreted under the lithosphere. Models of partial melting in plumes highlight the role that small degree partial melting may play in generating nephelinitic magmas away from the region of major picritic melting [42]. A model for secondary enrichment of a compacting sub-lithospheric accreted plume head (Fig. 5b) resulting in NSF mantle has been presented previously to account for the Pb isotopic data for the Cameroon line basalts [19]. Clearly, several scenarios can be envisaged that involve small melt fractions that upon migration will metasomatize the upper mantle near the base of the lithosphere at around the time of its growth and then migrate relative to the ridge (Fig. 5c) as the lithosphere ages. Melts from NSF mantle may not survive as erupted lavas close to ridges or in major plumes in regions of thin lithosphere because

Table 3
Partition coefficients used in melting calculations

| Phase | Olivine | | Clinopyroxene | | Orthopyroxene | | Garnet | | Amphibole | | Phlogopite | | Sulfide | |
|-------|--------------------|------|--------------------|--------|--------------------|---------|--------------------|----------|--------------------|---------|--------------------|---------|--------------------|------|
| | $D_{\text{min/q}}$ | Ref. | $D_{\text{min/q}}$ | Ref. | $D_{\text{min/q}}$ | Ref. | $D_{\text{min/q}}$ | Ref. | $D_{\text{min/q}}$ | Ref. | $D_{\text{min/q}}$ | Ref. | $D_{\text{min/q}}$ | Ref. |
| Rb | 0.0003 | 1 | 0.0004 | 5 | 0.0002 | 1,11,13 | 0.0002 | 11,14 | 0.023 | 15 | 1.7 | 6,13-15 | | |
| Ba | 5×10^{-6} | 2 | 0.0003 | 2 | 6×10^{-6} | 2 | 7×10^{-5} | 17,11 | 0.010 | 15 | 1.5 | 6,14 | | |
| Th | 7×10^{-6} | 2 | 0.0021 | 2 | 2×10^{-5} | 2 | 0.0021 | 17 | 0.001 | 5 | | | | |
| K | 2×10^{-5} | 1 | 0.001 | 5 | 0.0001 | 1,11,13 | 0.013 | 11 | 0.22 | 11 | 1.5 | 13,15 | | |
| U | 9×10^{-6} | 2 | 0.001 | 2 | 4×10^{-5} | 2 | 0.011 | 17 | 0.0012 | 2,11,15 | 0.0003 | 2,13 | | |
| Nb | 5×10^{-5} | 3 | 0.0089 | 6,7 | 0.003 | 12 | 0.01 | 12 | 0.08 | 6 | 0.14 | 6 | | |
| La | 0.0002 | 3 | 0.054 | 7 | 0.0031 | 3 | 0.0007 | 11,12 | 0.075 | 11,15 | 0.003 | 15 | | |
| Ce | 7×10^{-5} | 3 | 0.086 | 7 | 0.0021 | 3 | 0.0026 | 11,12 | 0.11 | 11,15 | 0.021 | 13,15 | | |
| Pb | 0.0003 | 2 | 0.0075 | 2,8 | 0.0014 | 11,13 | 0.0003 | 17 | 0.019 | 11,15 | 0.0043 | 13 | 10 | 16 |
| Pr | 0.0003 | 4 | 0.15 | 5 | 0.0026 | 3 | 0.005 | 5 | 0.15 | 5 | | | | |
| Sr | 4×10^{-5} | 1,2 | 0.091 | 2,7 | 0.0007 | 2 | 0.0007 | 17,14 | 0.27 | 6,11,15 | 0.044 | 13-15 | | |
| Nd | 0.0003 | 3 | 0.19 | 7 | 0.0023 | 3 | 0.027 | 11,12,14 | 0.23 | 11,15 | 0.0063 | 13,15 | | |
| Sm | 0.0009 | 3 | 0.27 | 7 | 0.0037 | 3 | 0.22 | 11,12,14 | 0.32 | 11,15 | 0.0059 | 13,15 | | |
| Zr | 0.001 | 3 | 0.26 | 6,7,9 | 0.012 | 3 | 0.2 | 12 | 0.25 | 6 | 0.13 | 6 | | |
| Hf | 0.0029 | 3 | 0.33 | 7,8,10 | 0.019 | 3 | 0.23 | 5 | 0.3 | 5 | | | | |
| Eu | 0.0005 | 3 | 0.43 | 5 | 0.009 | 3 | 0.61 | 11,12 | 0.52 | 11,15 | 0.031 | 13,15 | | |
| Ti | 0.015 | 3,4 | 0.40 | 7,10 | 0.086 | 3 | 0.6 | 12 | 0.95 | 6 | 0.98 | 6 | | |
| Gd | 0.0011 | 3 | 0.44 | 5 | 0.0065 | 3 | 1.2 | 11,12 | 0.53 | 11,15 | 0.0082 | 15 | | |
| Dy | 0.0027 | 3 | 0.44 | 7 | 0.011 | 3 | 2.0 | 11,12 | 0.50 | 11,15 | 0.026 | 15 | | |
| Y | 0.0082 | 3 | 0.47 | 7 | 0.015 | 3 | 2 | 5 | 0.54 | 6 | 0.03 | 5 | | |
| Ho | 0.01 | 5 | 0.4 | 5 | 0.016 | 3 | 2.5 | 5 | 0.5 | 5 | 0.03 | 5 | | |
| Er | 0.0109 | 3 | 0.39 | 7 | 0.021 | 3 | 3.3 | 11,12 | 0.46 | 11,15 | 0.030 | 15 | | |
| Yb | 0.024 | 3 | 0.43 | 7 | 0.038 | 3 | 6.4 | 11,12 | 0.50 | 11,15 | 0.030 | 15 | | |

References and notes: ¹[51], ²[31], ³[52], ⁴[53], ⁵interpolated, ⁶[54], ⁷[33], ⁸[28], ⁹[45], ¹⁰[47], ¹¹[34], ¹²[35], ¹³[46], ¹⁴[48], ¹⁵[49], ¹⁶[50], ¹⁷[32].

they will be diluted in larger degree (less enriched) partial melts that also form in those environments. However, the degree of partial melting in plumes is predicted to decrease as a function of the thickness of lithosphere or mechanical boundary layer [43]. Therefore, NSF mantle that survives and is transported away from the vicinity of a ridge melt zone may be preferentially resampled in regions of older, thicker lithosphere by smaller degrees of partial melting at greater depth [9,43,44].

4. Constraints on the generation of NSF mantle from trace element partition coefficients

Experimental partition coefficients for garnet (gt), orthopyroxene (opx) and olivine (ol) (Table 3) indicate that they are not capable of fractionating Ce/U/Pb ratios greatly, whereas the D s for clinopyroxene (cpx) define a broad range with approximate values of $10^{-4} < U < 10^{-2} \approx Pb < 10^{-1} \approx Ce$. The variability in Nb/U, Ce/U, Ce/Pb, U/Pb, Ba/Ce, Ba/Nb, Ba/Rb and K/U in a liquid as a function of degree of batch melting (F) of different assemblages is illustrated in Fig. 6. Similar results are obtained using cumulative products of Rayleigh fractional melting. In general, only higher quality recently determined partition coefficients have been used (Table 3), based either on experimental data or on isotope dilution measurements of separated minerals from peridotite xenoliths. For the purposes of this paper, the compilation in Table 3 has been made from selections of data that showed the greatest consistency, with a prejudice of rejecting higher D s.

The small range in Ce/U in OIB (Table 2) is difficult to reconcile with the larger variability found for Ce/Pb and U/Pb, since the bulk distribution coefficients should be closer for U and Pb, and for Ce and Pb, than for U and Ce (Table 3) and Fig. 6). All combinations of gt, cpx, opx and ol require $> 1\%$ for F to minimize Ce/U fractionation. Higher gt/cpx ratios also serve to minimize Ce/U fractionation. No combination of ol, cpx, opx and gt generates liquids with higher Ce/Pb than their source. This is hardly surprising, given the consistency of Ce/Pb in many basalts [3]. The fractionation in Ce/Pb found in regions of old lithosphere must

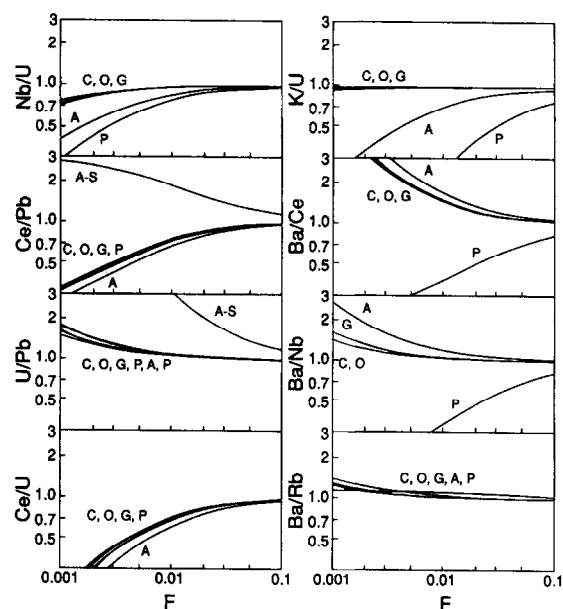


Fig. 6. Plot of incompatible trace element ratios vs. melt fraction for a batch melting model with the following assemblages: C = 5% cpx, 95% ol; O = 25% opx, 5% cpx, 70% ol; G = 2% gt, 25% opx, 5% cpx, 68% ol; P = 2% phl, 2% gt, 25% opx, 5% cpx, 66% ol; A = 2% amp, 2% gt, 25% opx, 5% cpx, 66% ol; A-S = 0.2% su, 2% amp, 2% gt, 25% opx, 5% cpx, 65.8% ol. All calculated assuming the D values given in Table 3.

therefore be brought about by minor phases only present at small degrees of partial melting. Similarly, the K/U ratios in MORB are relatively uniform (Table 2), a feature inferred to reflect similar bulk D for K and U during MORB melt production [1]. However, the K/U ratios in OIB are more variable (Table 2) and can be extremely low, associated with marked U enrichment and high Ce/Pb in the case of the Cape Verdes, Trinidad and the Cameroon line (Fig. 1 and Fig. 2d and 7). As with Ce/Pb, some minor phase must exist at small degrees of partial melting that fractionate K from U and that is more prevalent in enriched OIB (NSF) sources than in MORB sources (Fig. 7).

Such fractionations in enriched continental mantle-derived magmas have been ascribed to the importance of potassic phases, such as feldspar and phlogopite (phl), in the sub-continental lithospheric mantle [55,56]. However, Ba/Ce is surprisingly uniform in OIB compared with MORB (Table 2 and Fig. 2e). This is the opposite of that expected if phlogopite or

feldspar fractionate K because Ba tends to partition into these minerals [57] (Table 3 and Fig. 6). The most likely residual phase that could fractionate K strongly without affecting Ba/Ce ratios so greatly is amphibole (amp) [13] (Table 3 and Fig. 6). The importance of amp as opposed to phi as a storage site for H₂O in the upper mantle has been proposed previously [58]. However, any combination of ol, opx, cpx, gt and amp will generate a bulk *D* for Ba that is less than that for Ce (Fig. 6). That Ba/Ce does not vary with Ce concentration in OIB (Fig. 2e) is inconsistent with the results of such models. Therefore, unfractionated Ba/Ce ratios provide evidence of an additional trace phase that is rendering Ba less incompatible in NSF mantle. Trace (< 0.3%) amounts of phlogopite (Fig. 6) would be sufficient. If the bulk *D* for Ba is equivalent to that of Ce, because of minor phi in NSF mantle, one would

expect to observe variability in Ba/U (and Ba/Nb) but no change in Ba/Ce with degree of partial melting, exactly as observed in OIB (Fig. 2e and 7).

No combination of silicates, carbonates, phosphates or oxides is capable of producing the depletion in Pb and fractionations in U/Pb and Ce/Pb. However, sulfide (su) is likely to fractionate both U/Pb and Ce/Pb, while maintaining only minor fractionation of Ce/U [59]. Experimental studies of Pb partitioning between silicate and sulfide liquids indicate a high *D* for Pb that is a function of oxygen fugacity [50]. Low U/Pb ratios have been measured in sulfide inclusions in diamonds [60]; sulfide is ubiquitous in mantle samples [61] and there is evidence that it fractionates Re/Os in basalt genesis [62]. If small degrees of partial melting leave amp and su as residual (or dense immiscible) phases, fractionations in K/U, U/Pb and Ce/Pb are to be

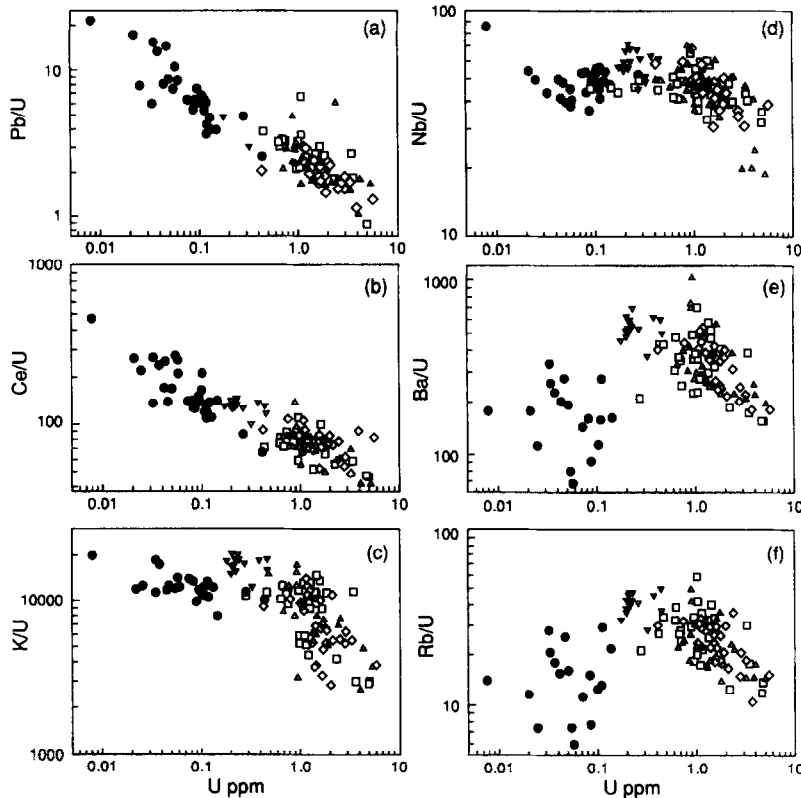


Fig. 7. Incompatible trace element ratios in MORB and OIB with U as the denominator, plotted against U concentration. Uranium would appear to be the most incompatible trace element in enriched OIB. Also note that the shape of the MORB field changes depending on the geometry relative to the OIB field, implicating mixing with OIB as a major contributor to the trace element variability, and in some cases uniformity in MORB. Data from Table 1 and [1–5,7,16,21,22,25].

expected. The predicted effects of batch melting a source with 5% cpx, 20% opx, 2% gt, 2% am, 0.2% ph, 0.2% su and 70.6% ol mimic many features of mantle-normalized incompatible trace element patterns of OIB from areas of old lithosphere (Fig. 1), including depletions in K and Pb. Titanium is also depleted and Zr enriched. Ba/Ce and Ce/U are only slightly fractionated, consistent with the observations for OIB. We propose that such melts enrich portions of the uppermost mantle and that this NSF mantle is subsequently remelted to form enriched OIB from regions of older lithosphere.

A significant result of such modelling is that U and Th are the most incompatible elements, more so even than Ba (Fig. 8). This runs contrary to mineral/melt partition coefficients for major mantle minerals [31,32], U–Th–Ra disequilibrium data for MORB and Hawaiian basalts [[63–65] and interpretations of trace element ratios in basalts more generally [2,4,5]. However, it is entirely consistent with the trace element ratios for OIB shown in Fig. 7. It can be seen that the ratios Rb/U, Ba/U, K/U, Nb/U, Pb/U and Ce/U all decrease with increasing U in enriched OIB. Since these trends are dominated by the data for enriched OIB, we conclude that U is notably more incompatible and/or Ba and Rb are less incompatible in the melting that produces enrichment in the *source* regions of OIB in areas of old lithosphere (NSF mantle) than is thought to be the case for MORB and OIB melt production. A similar feature has been noted for Th concentrations in OIB [36].

When the MORB field in Fig. 7 is collinear with the OIB array it defines a distinct correlated trend extending into the OIB field (e.g., Ce/U or Pb/U vs. U). When the MORB field plots at an acute angle to the OIB array the MORB trace element ratios display only a slight variability, plotting toward the center of the OIB field (e.g., K/U or Nb/U vs. U). When the MORB field plots entirely to one side of the OIB array it defines a broad field with no trend (e.g., Rb/U and Ba/U vs. U). These relationships are entirely consistent with contamination of MORB or the MORB source by OIB or the OIB source, as suggested by many others (e.g., [30,68]). When the vectors for contamination of MORB by OIB and for variability in OIB itself (whatever the cause) are not collinear, the MORB data define a scattered field.

On a plot of Ba/Ce ratio against $^{87}\text{Sr}/^{86}\text{Sr}$ (Fig. 9) the MORB data define a trend consistent with contamination by OIB-like components. There is also a tendency for Pb to be more radiogenic in MORB with low Ce/U. Therefore, these isotopic data lend support to the view that some N-MORB are contaminated by OIB components [30]. Furthermore, the homogeneity in isotopic composition for less incompatible elements such as Nd and Sr but greater heterogeneity in highly incompatible trace element ratios and Pb isotopic compositions of MORB may be explained by the influence of contamination by enriched small degree partial melts on a depleted peridotite source. Such an effect is found in spinel lherzolite xenoliths from the sub-continental lithospheric mantle for example [34].

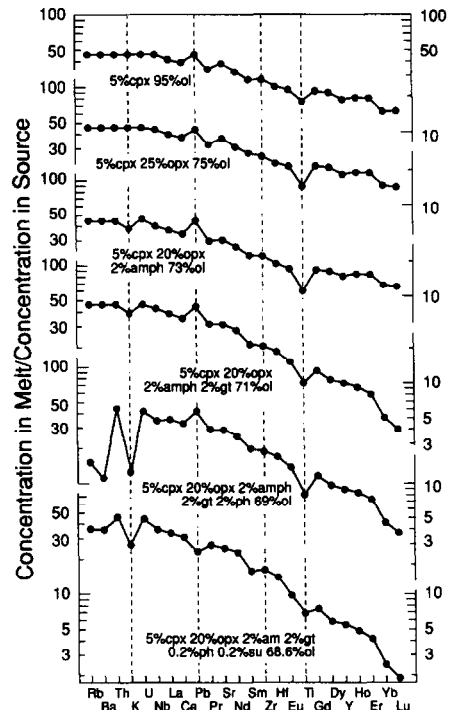


Fig. 8. Calculated trace element enrichments in 2% partial melts relative to their source compositions for different assemblages using the D values given in Table 3. Note the positive Pb anomaly for all assemblages unless sulfide is included, the strong depletion in Ba if too much phlogopite is present, the tendency for U to be the most incompatible element if minor phlogopite or amphibole are present and the similarity between the final pattern and that found in many enriched OIB (Fig. 1).

5. Effect of NSF mantle on large-scale mantle reservoirs

NSF mantle must become re-entrained in asthenospheric flow (Fig. 5d). It would then become a long-term heterogeneity producing isotopically enriched mantle, albeit greatly diluted, in a manner similar to that proposed for enrichment by subduction of oceanic crust [22,66] or erosion/delamination of sub-continental lithosphere [67]. Some OIBs, such as St. Helena, might inherit both their marked K depletions and high U/Pb (Fig. 1) from such longer term heterogeneities in the mantle. The striking features of such recycled NSF mantle would be LREE enrichment, higher U/Pb and Ce/Pb and lower K/U with normal Ba/Ce and Ce/U. This is distinctly different from the predicted effects of recy-

cling either continental or oceanic crust and it is significant that Ce/U and Ba/Ce in OIB are close to chondritic or primitive mantle values (Fig. 9 and Fig. 10), and yet not greatly fractionated by melting (Fig. 2 and Fig. 7). The variation in Ba/Nb ratio in OIB is often argued as reflecting the competing effects of recycling of Ba-depleted MORB on the one hand and Ba-enriched, Nb-depleted continental crust on the other [5,22,66]. However, the variability in both Ba/Ce and Ce/U in OIB is identical to that in Ba/Nb (Table 2). Furthermore, recycling models that advocate U enrichment or Pb depletion of MORB as the mechanism for generating radiogenic Pb in OIB (e.g., [22,39,66]) are difficult to reconcile with the fact that U/Pb variability in OIB is smaller than that in pristine MORB (Table 2).

Hydrothermally altered MORB, or its depleted

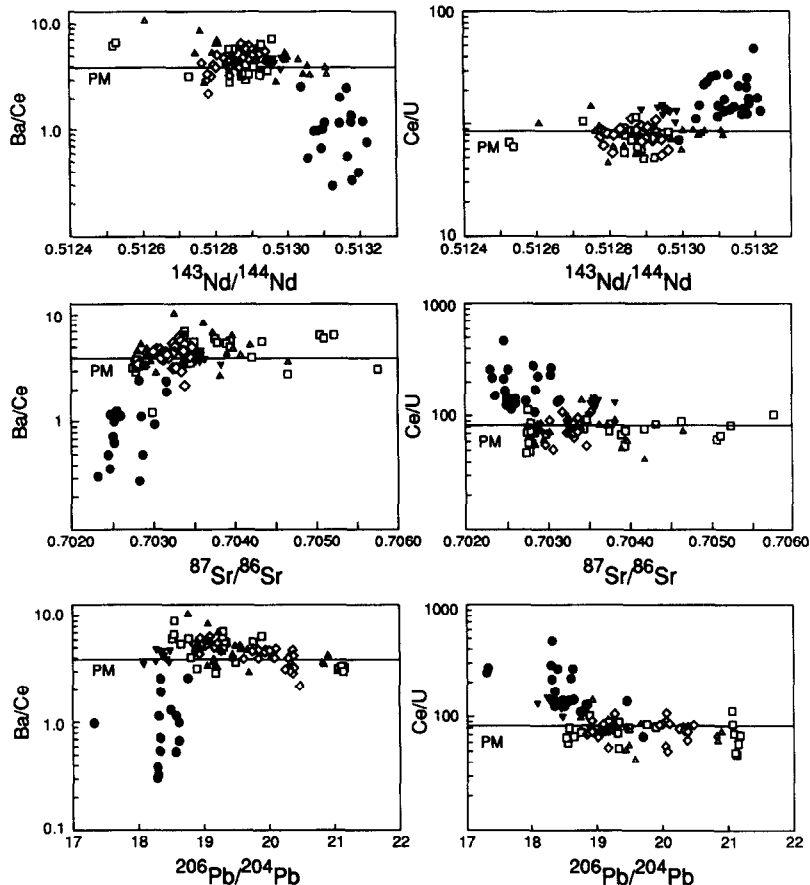


Fig. 9. Plots of Ba/Ce and Ce/U vs. Nd, Sr and Pb isotopic composition for MORB and OIB. Data from Table 1 and [1–5,7,9,16–26]. See text for discussion.

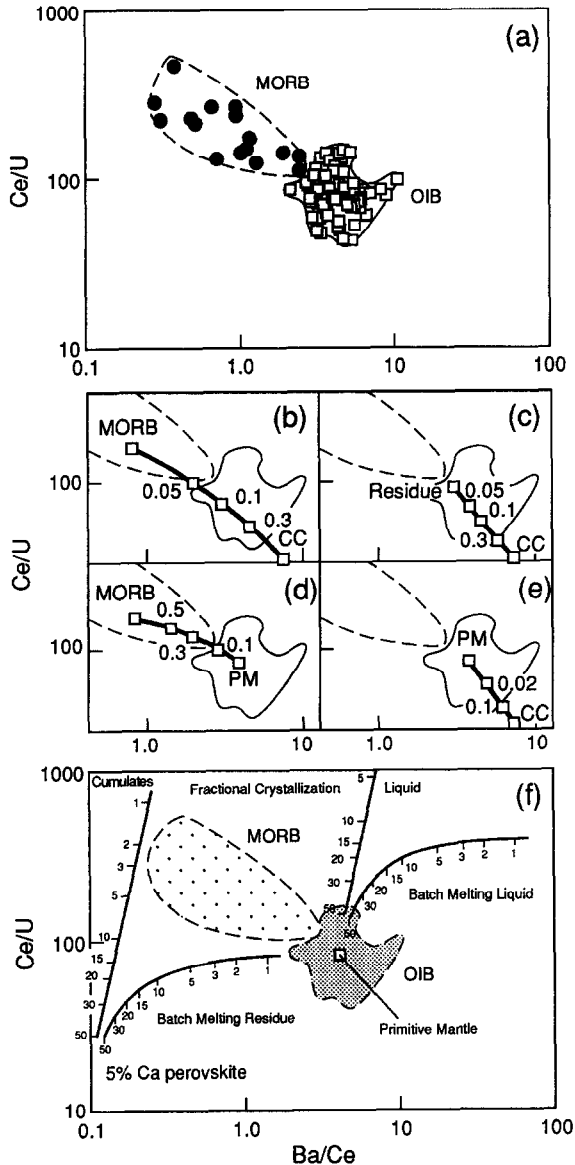


Fig. 10. (a) Ce/U vs. Ba/Ce for MORB (●) and OIB (□). Data sources as in Fig. 1. (b–e) The same data fields as in (a) but with the calibrated mixing trajectories of (b) average continental crust [71] and average MORB (calculated using data shown in (a)), (c) depleted altered MORB residue [66] and average continental crust, (d) average MORB and primitive mantle [5], and (e) average continental crust and primitive mantle [5]. (f) The same fields as in (a) but with the calibrated fractionation paths for an assemblage comprising 5% Ca perovskite and liquid, where the numbers define the fraction of liquid in simple batch melting and Rayleigh fractional crystallization, assuming Ba, Ce and U are perfectly incompatible in all other fractionating phases. Partition coefficients from [70].

residue after fluid/melt extraction in a subduction zone, should be closer in Ce/U and Ba/Ce to chondritic ratios [66]. Furthermore, if continental lithosphere were added in an appropriate amount and these heterogeneities became well mixed they might, coincidentally, generate a source with chondritic proportions. Samples with the highest Ba/Ce have unradiogenic Pb (Fig. 9d) consistent with recycling of small amounts of continental crust. Samples with the lowest Ba/Ce have radiogenic (HIMU) Pb (Fig. 9d) consistent with recycling of U-enriched ocean floor basalt. However, in order to balance the Ba/U/Ce in most OIB, about 10–30% of average continental crust must be combined with average MORB (Fig. 10b), or about 5–10% must be combined with the residual depleted altered MORB composition of Weaver [66] (Fig. 10c). These amounts would seem excessive given the considerable thickness of relatively unaltered basaltic oceanic crust and the fact that clastic sediments are diluted by siliceous oozes and carbonates that carry negligible Ba, U and Ce. The amount of basaltic/gabbroic ocean crust subducted can be estimated to be in the range $3\text{--}5 \times 10^{16}$ g yr⁻¹, whereas the current flux of subducting clastic sediment is estimated to be a maximum of 1×10^{15} g yr⁻¹ [D.K. Rea and L.J. Ruff, pers. commun., 1994]. Not even allowing for the fact that only a fraction of this sediment becomes entrained in the asthenosphere, this is too small to match the requirements of the Ba, U and Ce data for OIB. This is scarcely surprising. To consider this in somewhat different terms, it is improbable that primitive mantle, the ultimate source of depleted mantle, oceanic lithosphere and continental lithosphere can survive as a reasonably uniform composition sustained *dominantly* by the random admixing of two components (continental and oceanic lithosphere) with radically different compositions and survival times.

A more realistic scenario is one in which a significant component of OIB sources is mantle that has not undergone the major Ba/Ce/U fractionation found in MORB, the MORB source and the processes associated with subduction zone magmatism. Such mantle may be fractionated in Rb/Sr, Sm/Nd, Lu/Hf etc. by a prior history of melting in the garnet stability field. It may also be affected by minor amounts of enriched NSF mantle component with higher U/Pb and Ce/Pb and slightly lower

K/U, Ba/Nb and Ba/Ce. If such NSF mantle were recycled in diluted form (Fig. 5d), it would generate an 'end-member' composition with relatively radiogenic Pb and trace element characteristics that are similar to those of HIMU centers such as St. Helena. However, it would have near-chondritic Ba/Ce and Ce/U, and the contribution of material that is strongly fractionated in Ba/Ce and Ce/U (e.g., MORB and continental crust) would be relatively minor, preserving close to primitive mantle ratios for OIB source regions.

However, subducted MORB must be contributing to some degree in the trace element composition of the mantle. If we assume that the remainder of the source did indeed have primitive mantle relative concentrations [5] of Ba, Ce and U, the more scattered OIB data allow for a contribution to the OIB source of 10% of average modern unaltered MORB (Fig. 10d) and a greater contribution from altered MORB. If the absolute concentrations in the OIB source are depleted relative to primitive mantle, as seems inevitable, the amount of permissible recycled MORB contamination would be less. The difficulty with all these models based on Ba/Ce/U is that they do not explain the non-chondritic Nb/U of the mantle [3].

Finally, the data presented here place constraints on the processes that must have been involved in the early development of Earth's mantle. It has been proposed that the major element composition of the mantle can be explained by perovskite fractionation in a magma ocean [69]. However, it has also been argued that such a model is irreconcilable with the partitioning of Lu relative to Hf in Mg perovskite and the resulting fractionation expected in Lu/Hf [70]. The partition coefficients for Ba, Ce and U between Ca perovskite and silicate melt increase in the order Ba = 0.1, Ce = 4, U = 20 [70] and are so extreme that if it were an important phase during melting or fractional crystallization in the early Earth, the mantle could not maintain near-chondritic Ce/U and Ba/Ce. This is illustrated in Fig. 10f in which the effects of Rayleigh fractional crystallization and batch melting are shown starting with a primitive mantle composition. In contrast, majorite fractionation of the OIB source is not inconsistent with near-chondritic Ce/U and Ba/Ce. Garnet-like mineral phases in the early Earth and in modern melting

are not expected to greatly fractionate U, Ba or Nb from the LREE, unless the degree of partial melting is unrealistically small. The data presented here are therefore more readily accommodated by models in which the early Earth had at most a shallow magma ocean at pressures less than those required for phases such as Ca perovskite to be significant fractionating phases.

Acknowledgements

This paper has benefited enormously from discussion with, or criticism by P. Beattie, F. Frey, S. Goldstein, A. Hofmann, P. Kelemen, C. Langmuir, R. Lange, K. Mezger, P. Michael, S. Mukasa, K. O'Nions, M. Rehkämper, E. Stolper, Y. Zhang and an anonymous reviewer. The research was supported from National Science Foundation grant EAR 9205435 to ANH. [CL]

References

- [1] K.P. Jochum, A.W. Hofmann, E. Ito, H.M. Seufert and W.M. White, K, U and Th in mid-ocean ridge basalt glasses and heat production, K/U and K/Rb in the mantle, *Nature* 306, 431–436 1983.
- [2] A.W. Hofmann and W.M. White, Ba, Rb and Cs in the earth's mantle, *Z. Naturforsch.* 38a, 256–266 1983.
- [3] A.W. Hofmann, K.P. Jochum, M. Seufert and W.M. White, Nb and Pb in oceanic basalts: New constraints on mantle evolution, *Earth Planet. Sci. Lett.* 79, 33–45 1986.
- [4] H.E. Newsom, W.M. White, K.P. Jochum and A.W. Hofmann, Siderophile and chalcophile element abundances in oceanic basalts, Pb isotope evolution and growth of the earth's core, *Earth Planet. Sci. Lett.* 80, 299–313, 1986.
- [5] S.-S. Sun and W.F. McDonough, Chemical and isotopic systematics of oceanic basalts: Implications for mantle composition and processes, in: *Magmatism in the Ocean Basins*, A.D. Saunders and M.J. Norry, eds., *Geol. Soc. London Spec. Publ.* 42, 313–345, 1989.
- [6] J.-F. Minster and C.J. Allègre, Systematic use of trace elements in igneous processes, III. Inverse problem of batch partial melting in volcanic suites, *Contrib. Mineral. Petrol.* 68, 37–52, 1978.
- [7] G.R. Davies, M.J. Norry, D.C. Gerlach and R.A. Cliff, A combined chemical and Pb–Sr–Nd isotope study of the Azores and Cape Verdes hotspots: the geodynamic implications, in: *Magmatism in the Ocean Basins*, A.D. Saunders and M.J. Norry, eds., *Geol. Soc. London Spec. Publ.* 42, 231–255, 1989.

- [8] S.R. Hart, The DUPAL anomaly: A large scale isotopic mantle anomaly in the Southern Hemisphere, *Nature* 309, 753–757, 1984.
- [9] A.N. Halliday, G.R. Davies, D.-C. Lee, S. Tommasini, C. Paslick, J.G. Fitton and D.E. James, Lead isotopic evidence for young trace element enrichment in the oceanic upper mantle, *Nature* 359, 623–627, 1992 (correction, *Nature* 362, 184, 1993).
- [10] R.G. Mitchell-Thomé, *Geology of the South Atlantic Islands*, Borntraeger, Berlin, 1970.
- [11] R.G. Mitchell-Thomé, *Geology of the Middle Atlantic Islands*, Borntraeger, Berlin, 1976.
- [12] K.O. Emery and E. Uchupi, *The Geology of the Atlantic Ocean*, Springer, New York, 1984.
- [13] J.G. Fitton and H.M. Dunlop, The Cameroon line, West Africa and its bearing on the origin of oceanic and continental alkali basalt, *Earth Planet. Sci. Lett.* 72, 23–38, 1985.
- [14] J.G. Fitton, The Cameroon line, West Africa: a comparison between oceanic and continental alkaline volcanism, in: *Alkaline Igneous Rocks*, J.G. Fitton and B.G.J. Upton, eds., *Geol. Soc. London Spec. Publ.* 30, 273–291, 1987.
- [15] D.A. Chaffey, R.A. Cliff and B.M. Wilson, Characterization of the St. Helena magma source, in: *Magmatism in the Ocean Basins*, A.D. Saunders and M.J. Norry, eds., *Geol. Soc. London Spec. Publ.* 42, 231–255, 1989.
- [16] D.C. Gerlach, R.A. Cliff, G.R. Davies, M. Norry and N. Hodgson, Magma sources of the Cape Verdes archipelago: Isotopic and trace element constraints, *Geochim. Cosmochim. Acta* 52, 2979–2992, 1988.
- [17] D.C. Gerlach, J.C. Stormer, Jr. and P.A. Mueller, Isotopic geochemistry of Fernando de Noronha, *Earth Planet. Sci. Lett.* 85, 129–144, 1987.
- [18] A.N. Halliday, A.P. Dickin, A.E. Fallick and J.G. Fitton, Mantle dynamics: a Nd, Sr, Pb and O isotopic study of the Cameroon line volcanic chain, *J. Petrol.* 29, 181–211, 1988.
- [19] A.N. Halliday, J.P. Davidson, P. Holden, C. DeWolf, D.-C. Lee and J.G. Fitton, Trace-element fractionation in plumes and the origin of HIMU mantle beneath the Cameroon line, *Nature* 347, 523–528, 1990.
- [20] J.G. Fitton, C.R.J. Kilburn, M.F. Thirlwall and D.J. Hughes, 1982 eruption of Mt. Cameroon, *Nature* 347, 523–528, 1990.
- [21] D.-C. Lee, A.N. Halliday, J.G. Fitton and G. Poli, Isotopic variations with distance and time in the volcanic islands of the Cameroon line: evidence for a mantle plume origin, *Earth Planet. Sci. Lett.* 123, 119–138, 1994.
- [22] C. Chauvel, A.W. Hofmann and P. Vidal, HIMU–EM: The French Polynesian connection, *Earth Planet. Sci. Lett.* 110, 99–119, 1992.
- [23] E. Ito, W.M. White and C. Göpel, The O, Sr, Nd and Pb isotope geochemistry of MORB, *Chem. Geol.* 62, 157–176, 1987.
- [24] W.M. White, A.W. Hofmann and H. Puchelt, Isotope geochemistry of Pacific mid-ocean ridge basalt, *J. Geophys. Res.* 92, 4881–4893, 1987.
- [25] M.O. Garcia, B.A. Jorgenson, J.J. Mahoney, E. Ito and A.J. Irving, An evaluation of temporal geochemical evolution of Loihi summit lavas: Results from Alvin submersible dives, *J. Geophys. Res.* 98, 537–550, 1993.
- [26] W.M. White and A.W. Hofmann, Sr and Nd isotope geochemistry of oceanic basalts and mantle evolution, *Nature* 296, 821–825, 1982.
- [27] M.G. Seitz, Uranium and thorium partitioning in diopside–melt and whitlockite–melt systems, *Carnegie Inst. Washington Yearb.* 72, 551–553, 1973.
- [28] E.B. Watson, D. Ben Othman, J.-M. Luck and A.W. Hofmann, Partitioning of U, Pb, Cs, Yp, Hf, Re and Os between chromian diopsidic pyroxene and haplobasaltic liquid, *Chem. Geol.* 62, 191–208, 1987.
- [29] T.Z. LaTourrette and D.S. Burnett, Experimental determination of U and Th partitioning between clinopyroxene and natural and synthetic basaltic liquid, *Earth Planet. Sci. Lett.* 110, 227–244, 1992.
- [30] W.M. White, $^{238}\text{U}/^{204}\text{Pb}$ in MORB and open system evolution of the depleted mantle, *Earth. Planet. Sci. Lett.* 115, 211–226, 1993.
- [31] P. Beattie, The generation of uranium series disequilibria by partial melting of spinel peridotite: constraints from partitioning studies, *Earth Planet. Sci. Lett.* 117, 379–391, 1993.
- [32] P. Beattie, Uranium–thorium disequilibria and partitioning on melting of garnet peridotite, *Nature* 363, 63–65, 1993.
- [33] S.R. Hart and T. Dunn, Experimental cpx/melt partitioning of 24 trace elements, *Contrib. Mineral. Petrol.* 113, 1–8, 1993.
- [34] D.-C. Lee, A.N. Halliday, G.R. Davies, E.J. Essene, J.G. Fitton and R. Temdjim, Melt enrichment of shallow depleted mantle: a detailed petological, trace element and isotopic study of mantle derived xenoliths and megacrysts from the Cameroon line, *J. Petrol.*, in prep., 1995.
- [35] P.B. Kelemen, N. Shimizu and T. Dunn, Relative depletion of niobium in some arc magmas and the continental crust: Partitioning of K, Nb, La and Ce during melt/rock reaction in the upper mantle, *Earth Planet. Sci. Lett.* 120, 111–134, 1993.
- [36] C.J. Allègre, P. Schiano and E. Lewin, Differences between oceanic basalts by multitrace element ratio topology, *Earth Planet. Sci. Lett.* 129, 1–12, 1995.
- [37] C.J. Allègre, B. Hamelin, A. Provost and B. Dupré, Topology in isotopic multispace and origin of chemical heterogeneities, *Earth Planet. Sci. Lett.* 81, 319–337, 1986–1987.
- [38] C.J. Allègre, B. Dupré and O. Brévar, Chemical aspects of formation of the core, *Philos. Trans. R. Soc. London A306*, 49–59, 1982.
- [39] B. Peucker-Ehrenbrink, A.W. Hofmann and S.R. Hart, Hydrothermal lead transfer from mantle to crust: the role of metalliferous sediments, *Earth Planet. Sci. Lett.* 125, 129–142, 1994.
- [40] S.J.G. Galer and R.K. O’Nions, Magma genesis and the mapping of chemical and isotopic variations in the mantle, *Chem. Geol.* 56, 45–61, 1986.
- [41] T. Plank and C.H. Langmuir, Effects of the melting regime on the composition of the oceanic crust, *J. Geophys. Res.* 97, 19749–19770, 1992.

- [42] P.J. Wyllie, Solidus curves, mantle plumes and magma generation beneath Hawaii, *J. Geophys. Res.* 93, 4171–4181, 1988.
- [43] S. Watson and D. McKenzie, Melt generation by plumes: a study of Hawaiian volcanism, *J. Petrol.* 32, 501–537, 1991.
- [44] D. McKenzie and R.K. O’Nions, Partial melt distributions from inversion of rare earth element concentrations, *J. Petrol.* 32, 1021–1091, 1991.
- [45] S.M. Kuehner, J.R. Laughlin, L. Grossman, M.L. Johnson and D.S. Burnett, Determination of trace element mineral/liquid partition coefficients in melilite and diopside by ion and electron microprobe techniques, *Geochim. Cosmochim. Acta* 53, 3115–3130, 1989.
- [46] J.D. Kramers, J.C.M. Roddick and J.B. Dawson, Trace element and isotope studies on veined, metasomatic and ‘MARID’ xenoliths from Bultfontein, South Africa, *Earth Planet. Sci. Lett.* 65, 90–106, 1983.
- [47] T. Dunn, Partitioning of Hf, Lu, Ti, and Mn between olivine, clinopyroxene and basaltic liquid, *Contrib. Mineral. Petrol.* 96, 476–484, 1987.
- [48] R.S. Cohen, R.K. O’Nions and J.B. Dawson, Isotope geochemistry of xenoliths from East Africa: Implications for development of mantle reservoirs and their interaction, *Earth Planet. Sci. Lett.* 68, 209–220, 1984 (and W.I. Ridley and J.B. Dawson, Lithophile trace element data bearing on the origin of peridotite xenoliths, ankaramite and carbonatite from Lashaine volcano, N. Tanzania, *Phys. Chem. Earth* 9, 559–569, 1975).
- [49] A.J. Stolz and G.R. Davies, Chemical and isotopic evidence from spinel lherzolite xenoliths for episodic metasomatism of the upper mantle beneath southeastern Australia, *J. Petrol. Spec. Lithosphere Iss.*, pp. 303–330, 1988.
- [50] H. Shimazaki and W.H. MacLean, An experimental study on the partition of zinc and lead between the silicate and sulfide liquids, *Mineral. Deposita* 11, 125–132, 1976.
- [51] A. Zindler and E. Jagoutz, Mantle cryptology, *Geochim. Cosmochim. Acta* 52, 319–333, 1988.
- [52] A.K. Kennedy, G.E. Lofgren and G.J. Wasserburg, An experimental study of trace element partitioning between olivine, orthopyroxene and melt in chondrules: equilibrium values and kinetic effects, *Earth Planet. Sci. Lett.* 115, 177–195, 1993.
- [53] T. Dunn and C. Sen, Mineral/matrix partition coefficients for orthopyroxene, plagioclase, and olivine in basaltic to andesitic systems: A combined analytical and experimental study, *Geochim. Cosmochim. Acta* 58, 717–733, 1994.
- [54] J. Adam, T.H. Green and S.H. Sie, Proton microprobe determined partitioning of Rb, Sr, Ba, Y, Zr, Nb and Ta between experimentally produced amphiboles and silicate melts with variable F content, *Chem. Geol.* 109, 29–49, 1993.
- [55] C.J. Hawkesworth, P.D. Kempton, N.W. Rogers, R.M. Ellam and P.W. van Calsteren, Continental mantle lithosphere and shallow level enrichment processes in the Earth’s mantle, *Earth Planet. Sci. Lett.* 96, 256–268, 1990.
- [56] J.M. Rosenbaum, Mantle phlogopite: a significant lead repository? *Chem. Geol.* 106, 475–483, 1993.
- [57] J. Guo and T.H. Green, Experimental study of barium partitioning between phlogopite and silicate liquid at upper mantle pressure and temperature, *Lithos* 24, 83–95, 1990.
- [58] P.J. Michael, The concentration, behavior and storage of H₂O in the sub-oceanic upper mantle: Implications for mantle metasomatism, *Geochim. Cosmochim. Acta* 52, 555–566, 1988.
- [59] A. Meijer, T.-T. Kwon and G.R. Tilton, U–Th–Pb partitioning behavior during partial melting in the upper mantle: implications for the origin of high mu components and the ‘Pb paradox’, *J. Geophys. Res.* 95, 433–448, 1990.
- [60] J.D. Kramers, Lead, uranium, strontium, potassium and rubidium in inclusion-bearing diamonds and mantle-derived xenoliths from southern Africa, *Earth Planet. Sci. Lett.* 42, 58–70, 1979.
- [61] J.P. Lorand, Are spinel lherzolite xenoliths representative of the abundance of sulfur in the upper mantle, *Geochim. Cosmochim. Acta* 54, 1487–1492, 1990.
- [62] J.L. Bircck and C.J. Allègre, Contrasting Re/Os fractionation in planetary basalts, *Earth Planet. Sci. Lett.* 124, 139–148, 1994.
- [63] K.H. Rubin and J.D. Macdougall, ²²⁶Ra excesses in mid-ocean ridge basalts and mantle melting, *Nature* 335, 158–161, 1988.
- [64] A.S. Cohen and R.K. O’Nions, Melting rates beneath Hawaii: Evidence from uranium series isotopes in recent lavas, *Earth Planet. Sci. Lett.* 120, 169–175, 1993.
- [65] F. Chabaux and C.J. Allègre, ²³⁸U–²³⁰Th–²²⁶Ra disequilibria in volcanics: a new insight into melting conditions, *Earth Planet. Sci. Lett.* 126, 61–74, 1994.
- [66] B.L. Weaver, The origin of ocean island basalt end-member compositions: trace element and isotopic constraints, *Earth Planet. Sci. Lett.* 104, 381–397, 1991.
- [67] D. McKenzie and R.K. O’Nions, Mantle reservoirs and ocean island basalts, *Nature* 301, 229–231, 1983.
- [68] J.-G. Schilling, Upper mantle heterogeneities and dynamics, *Nature* 314, 62–67, 1985.
- [69] C.B. Agee and D. Walker, Mass balance and phase density constraints on early differentiation of chondritic mantle, *Earth Planet. Sci. Lett.* 90, 144–156, 1988.
- [70] T. Kato, A.E. Ringwood and T. Irifune, Experimental determination of element partitioning between silicate perovskites, garnets and liquids: constraints on early differentiation of the mantle, *Earth Planet. Sci. Lett.* 89, 123–145, 1988.
- [71] S.R. Taylor and S.M. McLennan, *The Continental Crust: Its Composition and Evolution*, Blackwell, Boston, Mass., 1985.